Preparation of Cellulose Nanocrystals Bio-Polymer From Agro-Industrial Wastes: Separation and Characterization

Mazlita Y., H.V. Lee* and S.B.A. Hamid
Nanotechnology & Catalysis Research Centre (NanoCat), Institute of Postgraduate Studies, University Malaya, 50603 Kuala Lumpur, Malaysia

SUMMARY

Lignocellulosic biomass from oil palm agro-industrial waste is highly potential to be valorised into cellulose polymer in nanoscale, which is useful for various applications. The present study discussed the synthesis of cellulose nanocrystal (CNC) from oil palm trunk (OPT) biomass *via* chemical-sonication process. The effect of pretreated alkali-bleached OPT and H_2SO_4 acid hydrolysed (40% and 60% w/w) cellulose were investigated by utilizing X-ray diffraction (XRD), Fourier transform infrared spectroscopy (FTIR), scanning electron microscopy (SEM), transmission electron microscopy (TEM) and thermogravimetric analysis (TGA). Biomass crystallinity, thermal stability and chemical functional group suggested that the pretreatment process has successfully isolated cellulose from OPT, which indicated the removal of lignin, hemicellulose and impurities from the palm fibers. Furthermore, SEM and TEM images revealed that CNC40 and CNC60 were observed in rod-shaped structure with the dimension of 100.00 nm (L) × 27.50 nm (d) and 95.00nm (L) × 25.00nm (d), respectively, and corresponded to the aspect ratio of 3.63 and 3.80, respectively. In the presence of sonication condition, the study suggested that both 40 and 60%w/w of H_2SO_4 rendered active effect for acid depolymerisation of cellulose at 45 °C and 15 min of time. Thus, this can concluded that milder acid (40%w/w) was able to produce cellulose in nanosizes under mild operating condition with the assistant of sonication effect.

Keywords: Nanocellulose, Lignocellulosic biomass, Hydrolysis, Depolymerisation, Acid catalyst

1. INTRODUCTION

To date, Malaysia is one of the world's primary palm oil producers that have been taking steps to promote the use of palm-derived energy and chemicals[1,2]. Oil palm biomass is a potential renewable resource which can contribute to the energy sustainability of the country as well as chemicals supply. This may minimise the negative impacts of petroleum combustion to the environment. Lignocellulosic biomass from oil palm are an inexpensive and readily available fiber source throughout the year[3]. This lignocellulosic resource mainly composed of cellulose, hemicellulose and lignin, which are categorized into carbohydrate and aromatic polymer which contributed to various applications based on its composition[4].

Among the bio-components present in oil palm biomass, cellulose is the primary structural building block of trees, which can be extracted for pulp and paper industry. Cellulose is a polymeric carbohydrate that contains many monosaccharide units covalently bonded to each other. This polymer is a linear chain of anhydro-glucose monomer units connected through 1,4 β-linkages. The compact structure of cellulose mainly contributed by the linkage of intra- and inter-hydrogen bond, which created a spectacular mechanical strength to protect the plant structure[5].

Lately, cellulose in nanodimension has been getting attention by various industries due to its superior characteristic as a green polymer nanomaterial. The major advantages of nanocellulose are including excellent mechanical strength, non-toxic and biodegradability and high availability to diverse surface functionalities for different applications. With all these superior properties, nanocellulose has a great potential in applications such as strength enhancers in paper, as additives to composites, polymer reinforcement, films and barrier coating, water treatment, oxygen barriers for food packaging, electronics, cosmetic, pharmaceuticals and biomedical devices (e.g. scaffolds in tissue engineering, artificial skin and cartilage, wound healing and vessel substitutes)[6,7].

To produce nanocellulose from lignocellulosic biomass, the complexity of the biomass structure needs to be ruptured so that the accessibility of cellulose in the plant fibres can be increased for depolymerisation process[8]. Ideally, chemical treatment is the most crucial route to obtain

*Corresponding author: leehweivoon@um.edu.my

nanoscale cellulose from the complex biomass. Various methods have been used to produce nanocellulose material from lignocellulosic biomass, this included acid, alkali, organosolv and ionic liquid treatment[8,9,10]. During biomass pretreatment process, the used of potassium hydroxide (KOH) solution make polymers (lignin, hemicellulose and cellulose) swelling, which partially breaking of inter- or intra hydrogen bonding from biomass structure occurred. The less ordered biomass structure lead to an increment of the active surface area (increase the number of available hydroxyl group) and accessibility to solvents for further hydrolysis process. Conventionally, acid sulphuric (H_2SO_4) or acid hydrochloric (HCl) were used for depolymerisation processing which acid will be the hydrolytic cleave, the glycosidic linkages between the two anhydroglucose units, dissolving the cellulose amorphous region and increase cellulose crystallinity[11].

To date, there are only several group of researchers reported on the extraction of microcrystalline cellulose (MCC) and nanocellulose (NC) from oil palm biomass resources, such as oil palm empty fruit bunch (OPEFB) and mesocarp oil palm fibres (MOPF)[4,12-15]. Typically, for every tonne of fresh fruit bunches (FFB) processed, 200 kg of empty fruit bunches (EFB), 670 kg palm oil mill effluent (POME), 120 kg of mesocarp oil palm fibers (MOPF), 70 kg shell and 30 kg palm kernel cake (PKC) are produced[16]. Both EFB and MOPF consisted of high content of cellulose fibres (around 35% and 32%, respectively), which are suitable to be transformed into value added products. To the best of our knowledge, there is no study has been discussed for the characteristics of OPT derived nanocellulose. Oil palm trunk (OPT) also considered as a potential cellulose resource which can be collected during replanting activities. About 41% of cellulose can be extracted from the trunk, which contains high cellulose content as EFB and MOPF[17]. Therefore, synthesis of cellulose nanocrystallite (CNC) from oil palm trunk (OPT) *via* a chemical route was performed. This process involved a two steps-treatment: (i) separation of non-cellulosic contents (hemicellulose and lignin) from OPT, (ii) acid depolymerise of synthesized cellulose to nanocellulose. Furthermore, the physicochemical properties of OPT-derived nanocellulose were discussed herein.

2. MATERIALS AND METHODS

2.1 Materials

Oil palm trunk (OPT) biomass was obtained from the Malaysian Palm Oil Board (MPOB), Malaysia. The chemicals used for biomass pretreatment and acid hydrolysis, such as potassium hydroxide (KOH) 85%, hydrogen peroxide (H_2O_2) 37%, and sulphuric acid (H_2SO_4) 98%, were purchased from R&M Chemical.

2.2 Fractionation of Cellulose

20 g of oil palm trunk (OPT) biomass were mashed and sieved to OPT powder (150 μm of particle sizes) prior for soxhlet extraction treatment. Under soxhlet extraction, OPT was immersed into mixture of toluene (C_7H_8) and ethanol (C_2H_7OH) with a ratio of 2:1 for 6 h as mentioned in literature studies [18,19,20]. The dewaxed OPT was aged in 2 M KOH solution for 3 days with vigorous stirring under room temperature. The swelled OPT was then bleached by 10% (v/v) of hydrogen peroxide (H_2O_2) solution at 75 °C for several times until the fibre color change from dark brown to white was observed. The *soxhleted and* extracted cellulose slurry (named as CelluloseS) was rinsed for few times with deionized water until it reached neutrality.

2.3 Cellulose Nanocrystal (CNC) Synthesis

Cellulose nanocrystals (CNCs) were prepared by sonication assisted acid hydrolysis of OPT extracted cellulose slurry(CelluloseS). The extracted cellulose undergoes hydrolysis reaction by using sulphuric acid (H_2SO_4) with different concentration of 40% and 60% w/w at 45 °C within 15 min duration. After hydrolysis process, acid solution was removed from hydrolysed product and washed several times until the medium reaches neutrality. Subsequently, the slurry were treated with 40kHz sonication for 40 min sat (WUC-A03H, DAIHAN, Korea) to disperse nanofiber in water. Finally, the products were dried in the fridge overnight to obtain CNCs precipitate. The synthesised nanocellulose at acid concentration of 40% and 60% are annotated as CNC40 and CNC60, respectively. The characteristics of treated products were characterized by using X-Ray diffraction spectroscopy (XRD), Fourier transform infrared spectroscopy (FTIR), Transition Emission Microscopy (TEM) and Scanning Electron Microscopy (SEM) and Thermogravimetric analysis (TGA).

2.4 Characterization

2.4.1 X-Ray Diffraction (XRD)

The X-Ray diffraction (XRD) patterns of the OPT, CelluloseS, CNC40 and CNC60 were obtained within a 2 range from 5 to 40° by using Shimadzu diffractometer model XRD 6000,with CuK_α radiation at the operating voltage of 2.7 kW. The crystallinity index (CrI) of samples was calculated based on the intensity between (002) and (101) lattice diffraction peaks using Segal's method[21] (Eq. 1). I_{002} represents both crystalline and amorphous region of cellulose (maximum intensity at 2 = 22°) while I_{am} represents only amorphous phase (intensity of diffraction at 2 = 18°):

$$\text{CrI}\ (\%) = \frac{I_{002} - I_{am}}{I_{002}} \times 100\% \qquad (1)$$

2.4.2 Fourier Transform Infrared Spectroscopy (FTIR)

The FTIR spectra were recorded by using Perkin Elmer spectrometer (Spectrum

Two) in the range 4000-500 cm^{-1} with a scanning resolution of 4 cm^{-1}. Ground samples were mixed with potassium bromide (KBr) and then pressed into ultra thin transparent pellets for analysis.

2.4.3 Transmission Electron Microscopy (TEM)

The dimensions of hydrolysed cellulose (CNC40 and CNC60) were determined by using EVISA LEO Libra-120 electron micron at an acceleration voltage of 120kV. A drop of diluted CNC was deposited on the surface of copper grid and allowed to dry at room temperature. Aspect ratios of length to diameter (L/D) of treated samples (CNC40 and CNC60) were calculated based on the TEM measurement.

2.4.4 Field Emission- Scanning Electron Microscopy (FE-SEM)

The sample of CNCs, OPT and CelluloseS were mounted with conductive carbon tape for SEM viewing process. The prepared samples were observed *via* FE-SEM (Fei Quanta 200F) and operated at 10 kV and 100 Paunder low vacuum condition.

2.4.5 Thermogravimetric Analysis (TGA)

GA analysis of CNCs, OPT and CelluloseS were performed by using TGA Q-500 (TA Instruments, United States of America). Each sample (1 mg) was heated at 10 °C/min from 25 °C to 900 °C under nitrogen (N_2) gas purging at the flow rate of 200 mL/min.

3. RESULTS AND DISCUSSION

3.1 Morphological Analysis

Figure 1 shows the images of the visual observation for ground OPT (a), CelluloseS (b), and CNCs (c). OPT biomass (**Figure 1a**) appear as brownish pieces of fibres with roughness of the surface before chemical treatment. After chemical pretreatment with alkali solution and H_2O_2 bleaching, the cellulose fibre was successfully isolated from hemicellulose and lignin in OPT with fluffy-white-cotton-ball-like appearance (**Figure 1b**). Further acid treatment of extracted cellulose has depolymerised the cellulose polymer chain into nanodimension slurry. Visually, it is clearly shown that CNC has formed stable emulsion in water, meanwhile, after drying, the pulp was disintegrated into an individual form of powder (**Figure 1c**).

The SEM morphology study of OPT biomass at different processing treatments was further investigated by using SEM analysis and the changes of fiber fine structure was observed (**Figure 2**). SEM images clearly displayed significant changes of OPT's structure after being treated under alkali, bleaching and acid condition. Based on **Figure 2a**, palm trunk biomass showed bundles of individual fibres which was coated with extractive materials such as waxes, pectin, hemicellulose, lignin and other impurities. Wax and pectin acted as a protective layer for palm fiber surfaces[22], thus soxhlet extraction treatment was performed to remove this hydrophobic layer in order to increase the accessibility of cellulose towards chemical attack. **Figure 2b** showed the de-lignified and bleached CelluloseS from palm trunk biomass (OPT), it was observed that the treated fibre appeared in smoother phases as most of the non-cellulosic content and impurities were removed from the fiber surface *via* soxhlet extraction, delignification and bleaching. These processes has broken the lignocellulosic complex, solubilised the lignin and hemicellulose, increase porosity and surface area of hidden cellulose. Thus, the cellulosic fibres were clearly aligned and distributed individually between each other and make the cellulose more accessible to hydrolysis reaction to nanocellulose (**Figure 2c** and **2d**). The structures for both CNC40 and CNC60 showed the aggregations of cellulosic fibres were reduced. Furthermore, the presence of cellulose crystallites (in the form of rod-shape) indicating that the intra-fibrillar structure was disintegrated into individual cells as the amorphous region of cellulose has been decomposed.

The shapes and sizes of the synthesized nanocrystallite celluloses (CNCs) by 40 and 60% of H_2SO_4 are determined by using transmission electron microscopy (TEM). TEM images (**Figure 3**) clearly revealed the rod-shaped of cellulose crystallites with nanoscale widths. The dimensional measurements of CNCs were determined by studying the aspect ratio of length (L) to diameter (d)- L/d. CNC40 rendered aspect ratio of 3.63 with dimension scale of 100.00 nm (L) × 27.5 nm (d), while the CNC60 is in higher aspect ratio of 3.8 with dimension of 95.00 nm (L) × 25.00 nm(d). As the acid concentration increased from 40 to 60%, the aspect ratio was significantly increased with smaller width and length of CNC due to acid attack. This finding was supported by several studies, where 60% of H_2SO_4 is the optimum concentration for the hydrolysis of cellulose to nanocellulose[23].

3.2 Chemical and Crystallinity Analyses

XRD analysis was performed to investigate the crystalline behaviour of OPT biomass, extracted cellulose and nanocrystalline celluloses (CNC40 and CNC60). The XRD patterns of all samples showed major peaks at around 2θ=15.6°, 22.2° and 44.4°, which indicated the presence of cellulose I_β structure (**Figure 4**).The crystallinity index (CrI) is used to indicate the order of crystallinity for raw biomass and treated biomass. **Table 1** showed the CrI increased in the order of OPT <CelluloseS <CNC40 <CNC60, which was 37.37%, 68.35%, 72.10% and 73.17%, respectively using Segal's empirical method. It was noticeable that extracted cellulose consisted of higher crystallinity compared to palm trunk. This is due to removal of

Figure 1. Visual observation: (a) Oil palm trunk (OPT), (b) CelluloseS, and (c) CNCs

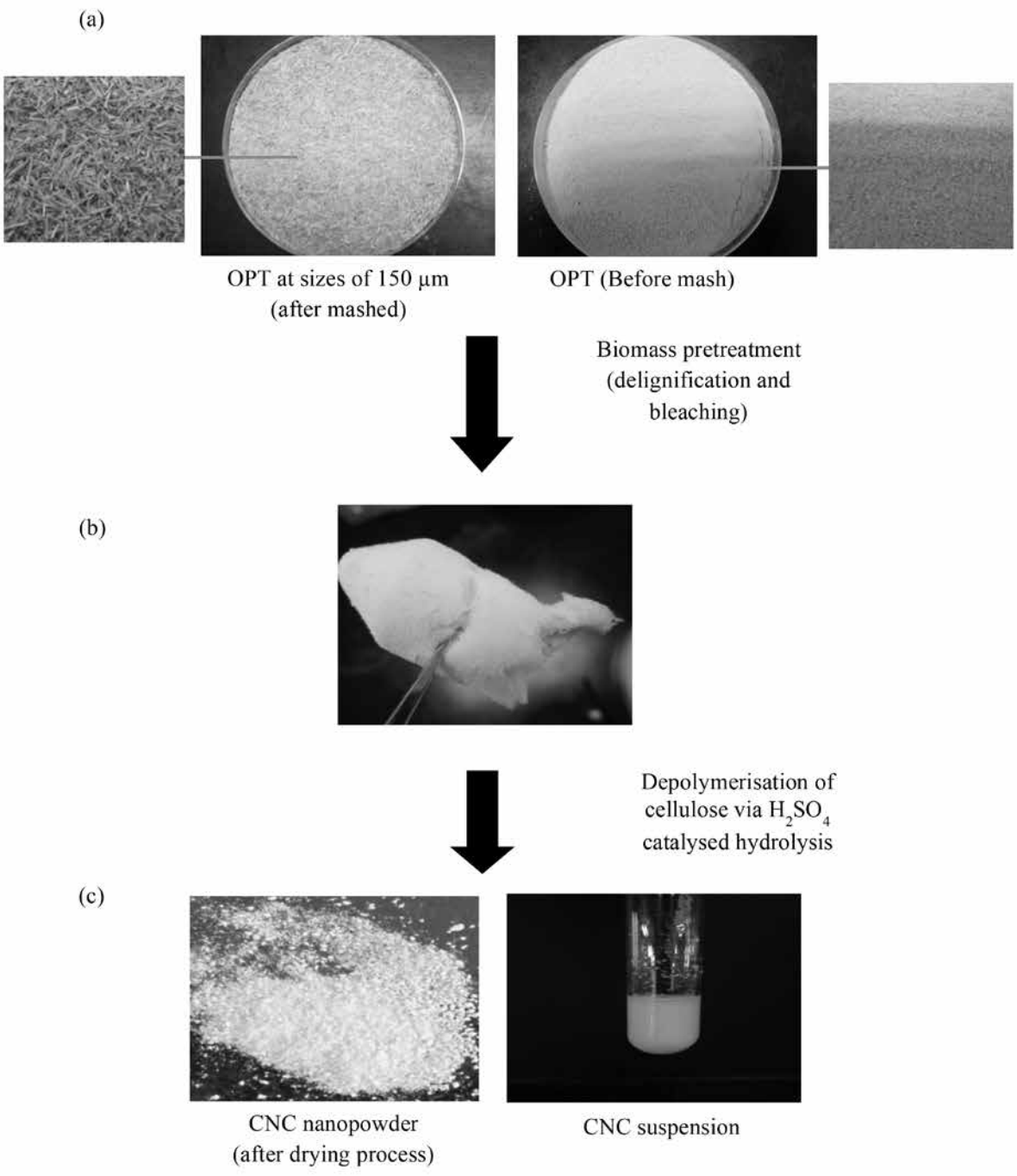

impurity and non-cellulosic content (lignin and hemicellulose) which has lead to the exposure of cellulose phases. The CrI of CNCs increased proportionally to the concentration of acid from 40% to 60% w/w of H_2SO_4. CNCs crystallinity is higher than CelluloseS indicated that the decay of amorphous region and rearrangement of the crystalline regions into a more ordered structure[24].

The changes in chemical surface of OPT biomass, CelluloseS (after biomass pretreatment) and CNCs (after acid hydrolysis) were evaluated by FTIR spectroscopy (**Figure 5**). FTIR spectra of the palm trunk (**Figure 5a**) showed an absorption peak at 1750 cm^{-1}, which is -C=O (saturated aldehyde) that attributed to vibration of xylan (hemicellulose)[25]. The respective peak was noticeable absence after the pretreatment process, which indicating

Figure 2. SEM micrographs of (a) OPT biomass, (b)CelluloseS, (c) CNC40, and (d) CNC60

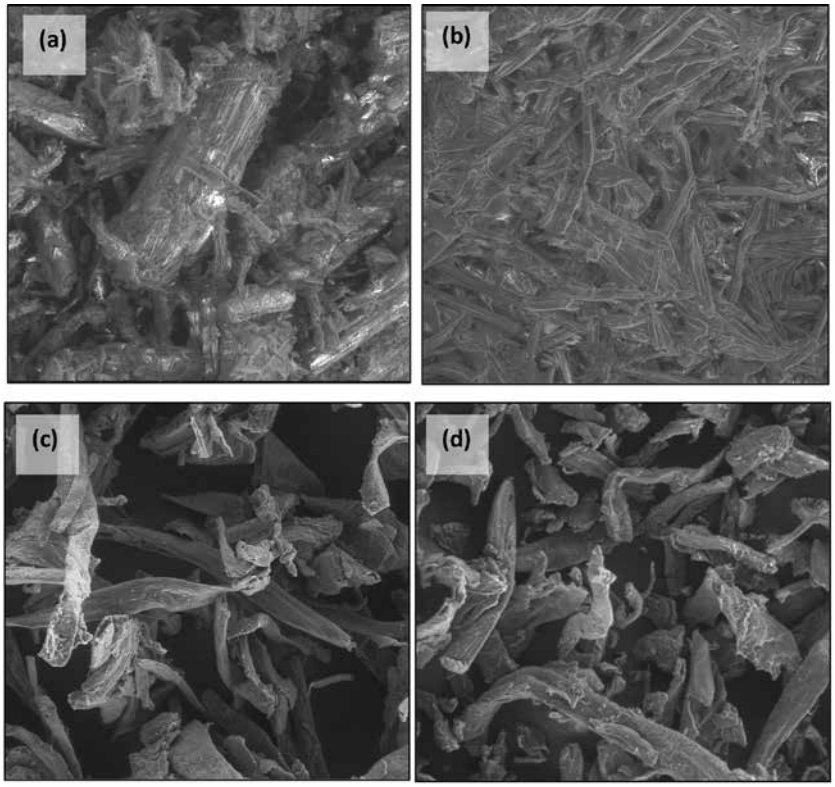

that hemicellulose was successfully removed from the complex biomass structures[26]. In addition, non-cellulosic lignin's chemical functional groups appeared at the band of 1505 cm^{-1} and 1500 cm^{-1}, which attributed to aromatic skeletal vibration in lignin[25], while FTIR band at 1235 cm^{-1} attributed to syringyl ring and CO stretch in lignin and xylan. These respective peaks also disappeared after the bleaching treatment, thus confirming that lignin and small part of hemicellulose were eliminated.

The FTIR spectrums for extracted cellulose (**Figure 5b**) and treated CNCs (**Figure 5c** and **5d**) showed similar patterns, suggesting that the chemical structure of nanocellulose remain unchanged after acid catalysed depolymerisation treatment. FTIR bands at 3344-3430 cm^{-1} attributed to -OH stretching, peaks at 2902 cm^{-1} attributed to C-H stretching, while the bands at around 1645 cm^{-1} raised

Figure 3. TEM micrographs of (a) Cellulose nanocrystallite, (b) CNC60, and (c) CNC40

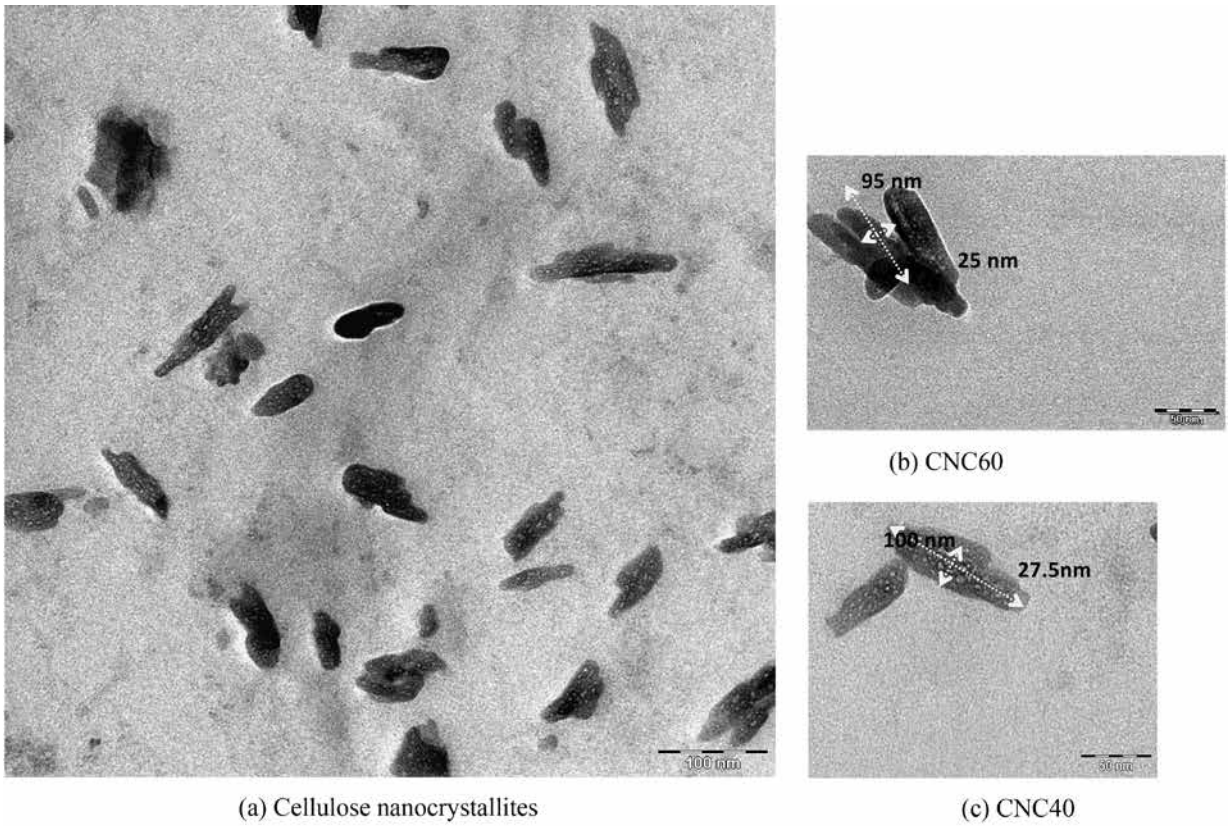

(a) Cellulose nanocrystallites

(b) CNC60

(c) CNC40

Figure 4. X-ray diffraction patterns for (a) OPT, (b) CelluloseS, (c) CNC40 and (d) CNC60

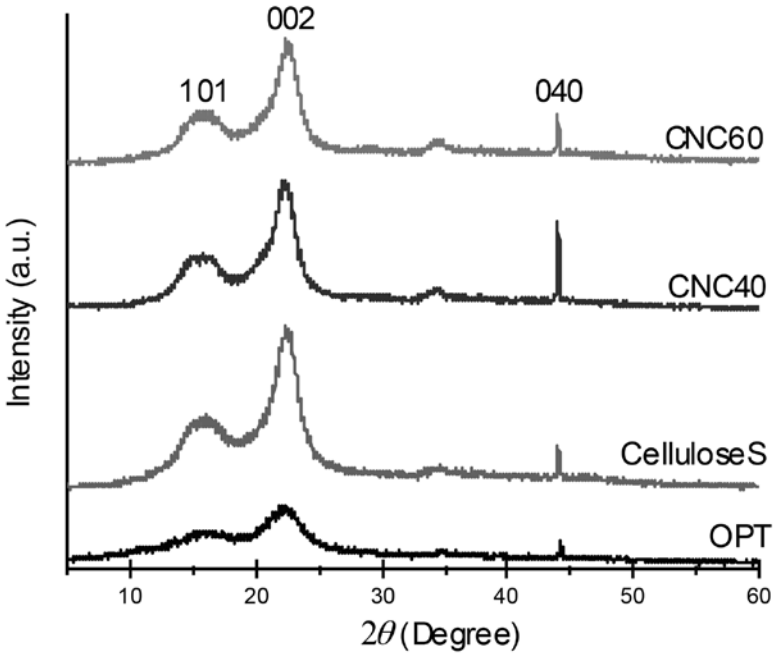

Figure 5. FTIR spectra of (a)OPT, (b) CelluloseS, (c) CNC40, and (d) CNC60

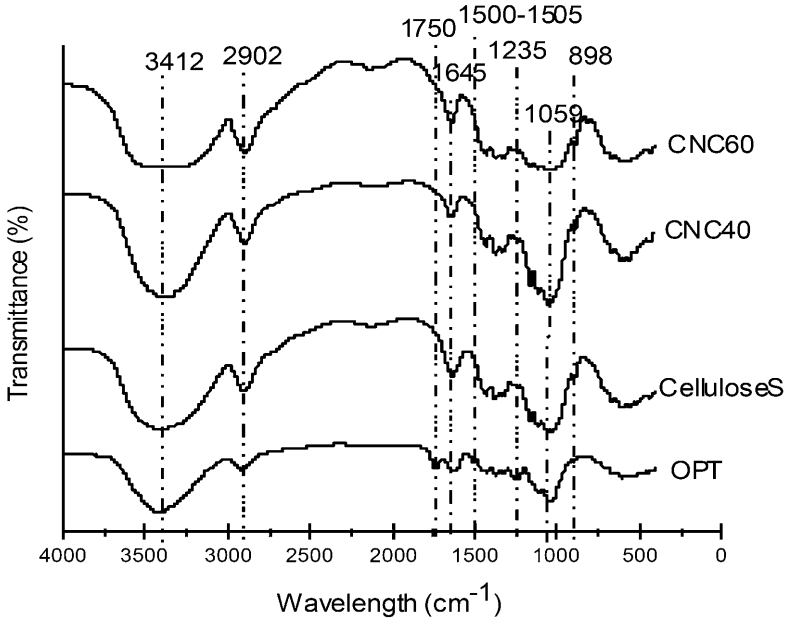

from bending vibrations of hydrogen bonded hydroxyl groups of cellulose and absorbed water[26,27]. Furthermore, the absorption bands at around 1058-1060 cm^{-1} attributed to C-O stretching and bands at 896-900 cm^{-1} indicated the presence of β-glycosidic linkages between glucose ring of cellulose chain[26,28-31]. Ideally, glycosidic linkage is to bond anomeric carbon atom of saccharides to form polysaccharides[32]. Thus, the presence of this bonding in the samples of CelluloseS, CNC40 and CNC60 indicated the presence of cellulose structure. Complimentary to SEM and TEM results, the pretreatment process successfully showed the presence of pure cellulose phase (removed of lignin and hemicellulose) and cleavage of glycosidic bond to reduce long chain of cellulose into nanocrystallite.

3.2.1 Thermal Properties

The thermal characteristics (stability and degradation during heating) of raw material (OPT), chemically-treated cellulose (CelluloseS) and nanocellulose (CNC40 and CNC60) were investigated by thermogravimetric analysis (**Figure 6** and **Table 2**). According to report by Poletto, the temperature at initial biomass decomposition is expected to be related to heating stability of biomass components and their difference in thermal stability, which can be attributed to the variation in chemical composition[33].

As shown in **Figure 6**, initial weight loss of samples at temperature of 70-80 °C indicating the removal of physisorbed water from the samples' surface[34]. The thermal degradation at

Table 1. Crystallinity index (CrI) of OPT, CelluloseS and CNCs at different stages of chemical treatment

Samples	2 (amorphous) (°)		2 (002) (°)		CrI (%)
	Degree	Intensity (I_{am})	Degree	Intensity (I_{002})	
OPT	18.45	337.01	22.00	538.06	37.37
CelluloseS	18.00	580.81	22.00	1670.23	67.07
CNC40	18.48	384.37	22.00	1377.53	72.10
CNC60	18.48	350.40	22.00	1306.25	73.17

temperature of 299 °C, 286 °C, 229 °C and 183 °C for OPT, CelluloseS, CNC40 and CNC60, respectively, was assumed as the starting decomposition temperature for all samples. These decomposition regions ranging from 180 °C to 400 °C was contributed to degradation of hemicellulose and lignin from OPT, decomposition and depolymerisation of CelluloseS and CNCs, correspondingly. As shown in **Table 2**, the order of starting decomposition temperature decreased in the trend of OPT>CelluloseS>CNC40>CNC60. The presence of hemicellulose and lignin in OPT consumed more energy to decompose the non-cellulosic content, especially of lignin, which require higher temperature (250 °C-400 °C) and longer time to break the heavily crossed linked aromatic rings[33]. This confirmed the existence of complex hemicellulose and lignin in OPT, which resulted in higher decomposition temperatures as compared to the CelluloseS. Cellulose in nanodimension (CNC40 and CNC60) showed significant differences of thermal decomposition behaviour from CelluloseS. The long-chain polymer structure of CelluloseS arranged in well order and strongly linked with hydrogen bonding consisted of higher thermal stability[35], this makes extra energy to cleave the chemical linkages. Low decomposition temperature of CNCs could be due to the smaller fiber dimension (nanometer scale) compared to microscale of cellulose, which lead to a larger surface area accessible to heat treatment[36]. Furthermore, sulphate content is one of the factors to reduce thermal stability of nanocellulose. As reported by several research groups, the presence of sulphate content (residual of H_2SO_4) adsorbed to outer surfaces of cellulose hydroxyl crystals will induce the decomposition of CNC chain under heating condition[12,37,38].

Figure 6. TGA thermogram for OPT,CelluloseS,CNC40 and CNC60

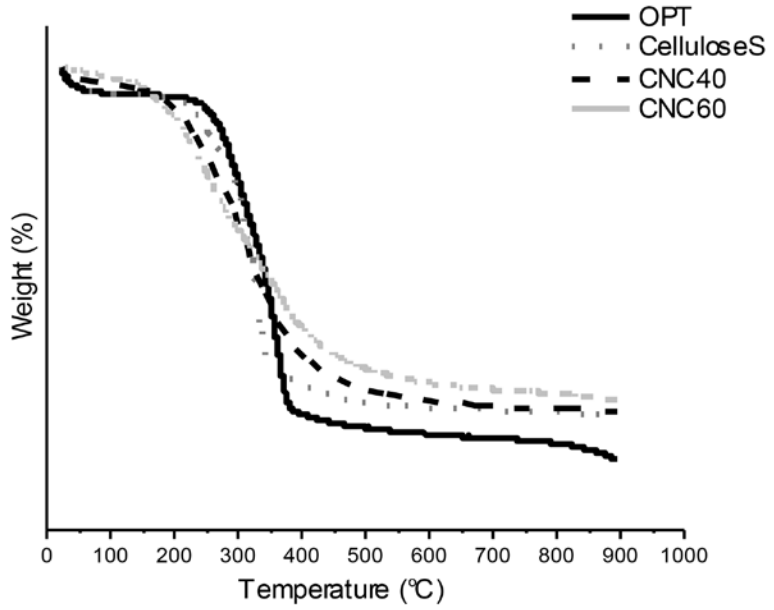

Table 2. TGA profile for OPT, CelluloseS, CNC40 and CNC60

Samples	Starting decomposition temperature (°C)
OPT	299
CelluloseS	286
CNC40	229
CNC60	183

3.2.2 Oil Palm-based Nanocellulose Synthesis Profile

In the present study, OPT derived cellulose nanocrystals was produced *via* sonication assisted chemical reaction. The presence of strong acid H_2SO_4 solution was initially dissociates in water to generate H^+ or H_3O^+ ions that responsible for cleavage of oxygen in glycosidic or intra- /intermolecular hydrogen bonding in cellulose chains[39]. Furthermore, acid hydrolysis was preferable to attack the amorphous (disordered) regions of cellulose chains as compared to crystalline (ordered) region, due to the high accessibility and low tensile strength of amorphous region. The produced CNCs from various concentration of acid: 40% and 60% rendered high crystallinity index (>70%) with aspect ratio (L/d)= >3.0 under shorter period of acid hydrolysis in the presence of bath sonication treatment. It was noticed that both acid concentration do not provided significant changes in key features of nanocrystalline cellulose. This was due to the presence of sonication treatment assisted in depolymerisation process when acid was promoted to mildly hydrolysed the cellulose chains. Thus, it can summarize that lower concentration of acid (40%) capable to produce high crystallinity of nanocrystalline cellulose at short period with the assisted sonication effect.

Table 3 showed the comparison profile of nanocellulose synthesis from different type of oil palm-based resources. Production of cellulose nanofibers (CNF) and microcrystalline cellulose from oil palm empty fruit bunch (OPEFB) was discussed[12-14]. Fahma *et al*. have fractionated nano-fibrillated cellulose (NFC) from OPEFB *via* sodium chlorite-potassium hydroxide-sulfuric acid ($NaClO_2$-KOH-H_2SO_4) chemical route. The particle sizes of nanocellulose were

Table 3. Summary of nanocellulose production from palm-based biomass[4]

Raw material	Final product	Treatment	Temperature (°C)	Time (h)	Crystallinity index (%)	Ref.
OPEFB	Cellulose nanofibers	Soxhlet extraction: C_2H_5OH:C_6H_6 (1:2 v/v) mixed solvent	80.1	48	54-59	Fahma *et al*. 2010
		$NaClO_2$ (pH 4-5)	70	1		
		KOH (6 wt.%)	20	24		
		H_2SO_4 (64 wt.%)	45	1		
OPEFB	Cellulose nanofibers	**Chemical treatment**			69	Jonoobi *et al*. 2011
		NaOH	70	180		
		sodium hydroxide-anthraquinone (12%+1%)	160	1.75		
		$NaClO_2$and CH_3COOH (1.25%+3%)	70	3		
		NaOH and H_2O_2 (1.5%+1%)	70	1.5		
		$NaClO_2$ and CH_3COOH (1.5%+3%)	70	1.5		
		Physical treatment				
		Mechanical grinding		0.25		
		High Pressure Homogenization	500 bar (pressure)	0.5		
OPEFB	Microcrystalline cellulose	HCl (2.5 N)	105	0.5	87	Mohamad Haafiz *et al*., 2013
		NH_4OH (5%)				
		Rotary ball mill				
MOPF	Cellulose nanowhiskers	NaOH (2 w/v.%)	80	2	70.90	Souza *et al*., 2013
		H_2O_2 (20%), v/v) and NaOH (4%, w/v)	55	1.5		
		H_2SO_4 (60%, w/w)	45	2.5		
OPT	Cellulose nanocrystallites	Soxhlet extraction: C_7H_8: C_2H_7OH (2:1)	Reflux temperature	6	72.10	Present Study
		KOH (2 M)	25	72		
		H_2O_2 (10%, v/v)	75	1		
		H_2SO_4 (40%, w/w) and sonication	45	0.25		

ranged in 1.96 nm to 2.51 nm with different treatment time (15 min, 30 min, 60 min, and 90 min). The crystallinity index of CNFs was decreased (59% to 54%) as the hydrolysis period increased from 15 min to 90 min, which indicated that most of the crystalline phase in cellulose fibers was further solubilise to smaller chain of cellulose[12].The isolation of cellulose nanofibers from OPEFB *via* chemo-mechanical route was done by Jonoobi and co-worker[13]. The OPEFB-derived cellulose was initially extracted *via* delignification-bleaching treatment was then followed by mechanical grinding and further break down into small particles by high pressure homogenizer. It was found that the use of chemo-mechanical processes to isolate nanofibers provide an easy method to produce cellulose nanofibers with higher crystallinity (69%) and better thermal stability compared to the acid hydrolysis technique[13]. Similar to Jonoobi[13] chemical-mechanical synthesis method, Mohamad Haafiz *et al*.[14] have successfully produced MCC from OPEFB *via* chemical route with the aid of mechanical treatment (rotary ball milling). The OPEFB was hydrolysed by using 2.5 N of hydrochloric acid (HCl) under 105 °C for 30 min with the pulp to liquor ratio of 1:20. After completion of acid hydrolysis, sample was washed several times before being proceed to neutralization by ammonium hydroxide (NH_4OH). The dried product was then grinded into fine powder by using rotary ball miller to produce MCC. The crystallinity index for OPEFB-MCC is 87% which is higher compared to raw OPEFB (80%) and commercial MCC (79%)[14]. These

studies indicated that the amorphous region of cellulose can removed by acid hydrolysis while preserving individual whisker/crystallite phases. As the crystallinity of cellulose is directly proportional to cellulose rigidity, thus this showed that higher crystallinity index of nanocellulose consisted of higher mechanical properties. Other than OPEFB from oil palm resource, pressed mesocarp oil palm fibers (MOPF) was successfully transformed into nanowhiskers cellulose *via* conventional pulping treatment. The nanocellulose product rendered the length (L) of 171.76 nm while the diameter (D) is average of 5.48 nm, with the aspect ratio (L/D) of 35.35 and crystallinity index of 70.90% [15].

4. CONCLUSIONS

Cellulose nanocrystals (CNCs) were successfully generated from oil palm trunk (OPT) lignocellulosic biomass *via* sonication assisted chemical treatments. The FTIR analysis revealed that lignin and hemicellulose (non-cellulosic contents) were successfully removed from OPT *via* alkali and bleaching treatments. Furthermore, TEM images indicated that acid hydrolysis is able to depolymerise cellulose micro-chain into nanocrystallites in which CNC40 and CNC60 rendered average dimensions in nano-length (<100 nm) and nano-dimension (<30 nm). This fact was further supported by XRD analysis, where the crystallinity (Crl) of CNCs were higher than CelluloseS, which indicates the exposure of crystalline phase as the amorphous region of cellulose was attacked by acid. Furthermore, CNCs showed lower thermal stability as compared to cellulose and OPT, which implied that nanocrystallites with higher surface area were easily exposed to heat. With the presence of sonication treatment, this study suggested that both 40 and 60% w/w of H_2SO_4 rendered active effect for acid depolymerisation of cellulose at 45 °C and 15 min of time with high crystallinity (>70%) and aspect ratio (L/d) >3.0. Thus, this can concluded that milder acid (40% w/w) was able to produce cellulose in nanosizes under mild operating condition with the assistant of sonication effect.

ACKNOWLEDGMENTS

The authors are grateful for the financial support of the Minister of Science, Technology and Innovation (MOSTI) e-ScienceFund (SF002-2015) and Postgraduate Research Grant Scheme PPP(PG079-2015) from University of Malaya.

REFERENCES

1. Shuit, S.H., Tan, K.T., Lee, K.T., and Kamaruddin, A.H. *Energy,* **34**(9), 2009, 1225-1235.
2. Sulaiman, F., Abdullah, N., Gerhauser, H., and Shariff, A. *Biomass and Bioenergy,* **35**(9), 2011, 3775-3786.
3. Shinoj, S., Visvanathan, R., Panigrahi, S., and Kochubabu, M. *Industrial Crops and Products,* **33**(1), 2011,7-22.
4. Yahya, M.B., Lee, H.V., and Hamid, S.B.A. *BioResources,* **10**(4), 2015, 7627-7639.
5. Lindman, B., Karlström, G., and Stigsson, L. *Journal of Molecular Liquids,* **156**(1), 2010, 76-81.
6. Brinchi, L., Cotana, F., Fortunati, E., and Kenny, J.M. *Carbohydr Polym,* **94**(1), 2013, 154-169.
7. Dufresne, A. *Materials Today,* **16**(6), 2013, 220-227.
8. Kumar, P., Barrett, D.M., Delwiche, M.J., and Stroeve, P. *Industrial and Engineering Chemistry Research,* **48**(8), 2009, 3713-3729.
9. Halib, N., Amin, M.C.I.M., and Ahmad, I. *Sains Malaysiana,* **41**(2), 2012, 205-211.
10. Lee, H.V., Hamid, S.B., and Zain, S.K. *Scientific World Journal,* 2014, 631013.
11. Morais, J.P.S., Rosa, M.d.F., Nascimento, L.D., do Nascimento, D.M., and Cassales, A.R. *Carbohydrate Polymers,* **91**(1), 2013, 229-235.
12. Fahma, F., Iwamoto, S., Hori, N., Iwata, T., and Takemura, A. *Cellulose,* **17**(5), 2010, 977-985.
13. Jonoobi, M., Khazaeian, A., Tahir, P.M., Azry, S.S., and Oksman, K. *Cellulose,* **18**(4), 2011, 1085-1095.
14. Mohamad Haafiz, M., Eichhorn, S., Hassan, A., and Jawaid, M. *Carbohydrate Polymers,* **93**(2), 2013, 628-634.
15. Souza, N., Pinheiro, J., Brígida, A., Morais, J., Filho, M.S., and Rosa, M. *Cellulose Nano Whiskers From Oil Palm Fibers*. Paper presented at the Embrapa Agroindústria de Alimentos-Artigo em anais de congresso (ALICE), 2013.
16. Aziz, A.A., Das, K., Husin, M., and Mokhtar, A. *Journal of Oil Palm Research,* **14**(2), 2002, 10-17.
17. Hameed, B.H., and El-Khaiary, M.I. *Journal of Hazardous Materials,* **154**(1–3), 2008, 237-244.
18. Abe, K., Iwamoto, S., and Yano, H. *Biomacromolecules, 8*(10), 2007, 3276-3278.
19. Abe, K., and Yano, H. *Cellulose,* **16**(6), 2009, 1017-1023
20. Kumar, A., Negi, Y.S., Choudhary, V., and Bhardwaj, N.K. *Journal of Materials Physics and Chemistry,* **2**(1), 2014, 1-8.
21. Segal, L., Creely, J., Martin, A., and Conrad, C. *Textile Research Journal,* **29**(10), 1959, 786-794.
22. Johar, N., Ahmad, I., and Dufresne, A. *Industrial Crops and Products,* **37**(1), 2012, 93-99.
23. Bondeson, D., Mathew, A., and Oksman, K. *Cellulose,* **13**(2), 2006, 171-180.
24. Howell, C., Hastrup, A.C.S., Jara, R., Larsen, F.H., Goodell, B., and Jellison, J. *Cellulose,* **18**(5), 2011, 1179-1190.
25. Lai, L.-W., and Idris, A. *BioResources,* **8**(2), 2013, 2792-2804.
26. Gibson, L.J. *J R Soc Interface,* **9**(76), 2012, 2749-2766.
27. He, W., Jiang, S., Zhang, Q., and Pan, M. *BioResources,* **8**(4), 2013, 5678-5689.
28. Alemdar, A., and Sain, M. *Bioresource Technology,* **99**(6), 2008, 1664-1671.
29. Hromádková, Z., Ebringerová, A., and Valachovič, P. *Ultrason Sonochem,* **5**(4), 1999, 163-168.

30. Rosa, M.F., Medeiros, E.S., Malmonge, J.A., Gregorski, K.S., Wood, D.F., Mattoso, L.H.C., Imam, S.H. *Carbohydrate Polymers,* **81**(1), 2010, 83-92.
31. Sheltami, R.M., Abdullah, I., Ahmad, I., Dufresne, A., and Kargarzadeh, H. *Carbohydrate Polymers,* **88**(2), 2012, 772-779.
32. Cabiac, A., Guillon, E., Chambon, F., Pinel, C., Rataboul, F., and Essayem, N. *Applied Catalysis A: General,* **402**(1–2), 2011, 1-10.
33. Poletto, M., Zattera, A.J., Forte, M.M.C., and Santana, R.M.C. *Bioresource Technology,* **109**(0), 2012, 148-153.
34. Cho, M.-J., and Park, B.-D. *Journal of Industrial and Engineering Chemistry,* **17**(1), 2011, 36-40.
35. Yang, H., Yan, R., Chen, H., Lee, D.H., and Zheng, C. *Fuel,* **86**(12–13), 2007,1781-1788.
36) Jiang, F., and Hsieh, Y.-L. *Carbohydrate Polymers,* **95**(1), 2013, 32-40.
37. Chen, Y., Liu, C., Chang, P.R., Cao, X., and Anderson, D.P. *Carbohydrate Polymers, 76*(4), 2009, 607-615.
38. Wang, N., Ding, E., and Cheng, R. *Polymer,* **48**(12), 2007, 3486-3493.
39. Yahya, M., Lee, H., Hamid, S.A., and Zain, S. *Polymer Research Journal,* **9**(4), 2015, 1-22.
40. Cherian, B.M., Pothan, L.A., Nguyen-Chung, T., Mennig, G., Kottaisamy, M., and Thomas, S. *J Agric Food Chem,* **56**(14), 2008, 5617-5627.